Oxidative dehydrogenation of isobutane over pyrophosphates catalytic systems

S.M. Al-Zahrani [a,*], N.O. Elbashir [a], A.E. Abasaeed [a] and M. Abdulwahed [b]

[a] *Chemical Engineering Department, King Saud University, Riyadh, Saudi Arabia*
E-mail: szahrani@ksu.edu.sa
[b] *SABIC Industrial Complex For Research and Technology, Riyadh, Saudi Arabia*

Received 9 September 1999; accepted 20 July 2000

The catalytic effect of metal pyrophosphates (i.e., $Mn_2P_2O_7$, $Ni_2P_2O_7$, CeP_2O_7, $Mg_2P_2O_7$, ZrP_2O_7, $Ba_2P_2O_7$, $V_4(P_2O_7)_3$ and $Cr_4(P_2O_7)_3$) on the oxidative dehydrogenation of isobutane to isobutene in the reaction temperature range of 400–600 °C has been investigated. CeP_2O_7 gives the highest isobutene yield and selectivity (71%), however, $V_4(P_2O_7)_3$ is the most active catalyst with an isobutane conversion of 33.5% at 500 °C. Increasing the reaction temperature results in higher isobutane conversions and lower isobutene selectivity. Reaction by-products are propylene, CO, CO_2 and traces of methane and ethylene. No oxygenate products are formed under the used reaction conditions. The sum of selectivities of CO, CO_2 and methane is approximately equal to that of propylene, indicating their formation from total oxidation of C_1 species accompanying the isobutane crack reactions. Working at temperatures higher than 550 °C, the homogeneous gas phase reactions become significant and the oxygen conversion reaches 100%.

Keywords: pyrophosphate catalyst, dehydrogenation of isobutane

1. Introduction

Making valuable products from light hydrocarbons is presently one of the major challenges for the petroleum and petrochemical industries. Dehydrogenation reactions are used in industry for the production of lower alkenes (e.g., ethene, propene, butene, isobutene, etc.) from their corresponding paraffins [1–4]. These reactions are reversible, therefore, the conversion is limited by thermodynamic equilibrium. Undesired cracking of the hydrocarbons occurs, due to the required high temperature. Besides coke deposition and short catalyst life, heat must be provided at these high temperatures for these endothermic reactions to proceed. This increases the production cost significantly. Many of these obstacles can be overcome by providing the heat necessary for the reaction via, *in situ*, oxidation of the hydrogen evolved as a product of pure dehydrogenation, usually with oxygen. The overall reaction, therefore, becomes exothermic and able to proceed at much lower temperatures, thus minimizing the formation of coke and cracking products. Another advantage of this reaction is that it is no longer limited by thermodynamic factor. This type of reactions is termed oxidative dehydrogenation (ODH) reaction.

Due to increased demand for methyl tertiary butyl ether (MTBE, is formed from isobutene and is used as an octane booster for gasoline), research on oxidative dehydrogenation of isobutane to isobutene is gaining momentum. A number of catalytic systems have been used for ODH of isobutane, such as metal pyrophosphates [5,6], rare earth metal phosphates [7], supported metal oxides [8–15], Dawson- and Keggin-type heteropolyanions [16–19]. Takita et al. [5,6] tested the pyrophosphates of Ag, Ni, Zn, Cr, Sn, Mg, Cu, Mn and Co at 450–550 °C for the ODH of isobutane to isobutylene using an isobutane-rich feed gas. They reported that among these catalysts the $Ni_2P_2O_7$ is the most selective catalyst with the isobutene selectivity reaching a maximum value of 82.2% at 550 °C. $Ag_4P_2O_7$ and $Zn_2P_2O_7$ were also effective but the isobutene selectivities were slightly lower than that of $Ni_2P_2O_7$. On the other hand, the selectivities obtained with $Co_2P_2O_7$, $Mn_2P_2O_7$, $Cr_4(P_2O_7)_3$ and $Mg_2P_2O_7$ are in the range of 60–70%. Oxidation to CO and CO_2 is promoted when $Cu_2P_2O_7$ and $Sn_2P_2O_7$ are used as catalysts. Rare earth metal phosphates ($CePO_4$, $LaPO_4$, YPO_4, $PrPO_4$, $NdPO_4$, $GdPO_4$, $ErPO_4$ and $YbPO_4$) were also used for oxidative dehydrogenation of isobutane [7]. Only $CePO_4$ and $LaPO_4$ were found to be effective. In both studies [5–7] the feed composition was 75% isobutane, 5% oxygen and 20% nitrogen, and the residence time was 11 s. The optimum oxygen concentrations for isobutene formation was found to be in the range 5–15 mol%. Further increase of oxygen concentration led to a decrease of isobutene selectivity.

In this paper, we report the experimental results on selective oxidative dehydrogenation of isobutane to isobutene over a number of metal (Mn, Ni, Mg and Cr) pyrophosphate catalysts reported by Takita et al. [5–7], however under different feed composition and residence time. In addition, other pyrophosphate catalysts containing Ce, Zr, Ba and V were also tested for comparison purposes. Samples of the XRD and FT-IR results (before and after reaction) are also presented.

* To whom correspondence should be addressed.

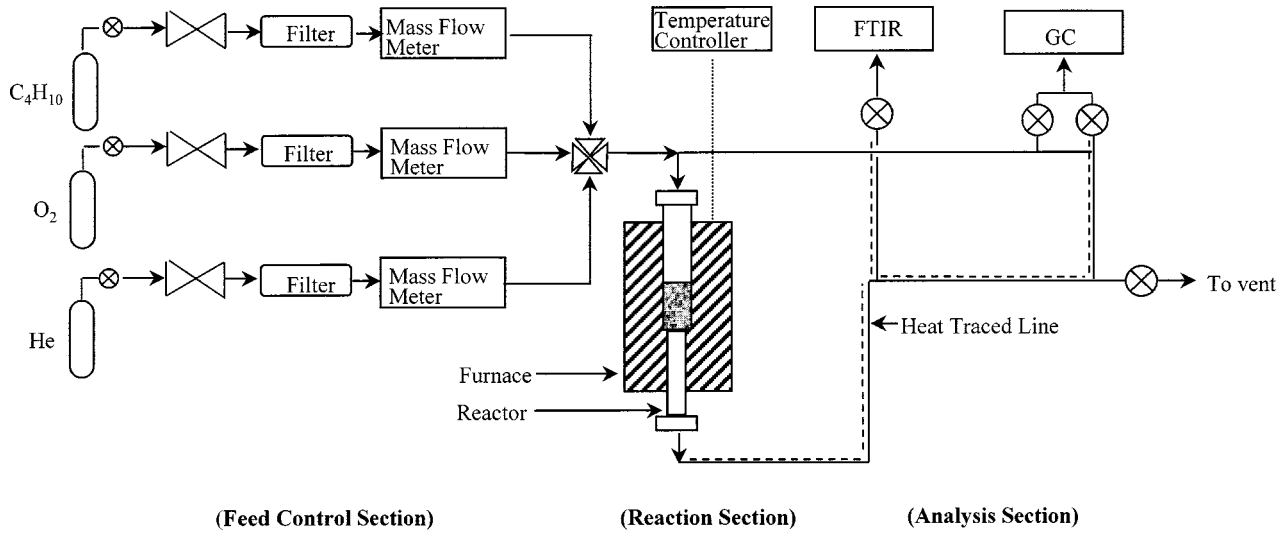

Figure 1. Schematic diagram of the experimental setup.

2. Experimental

2.1. Catalyst

The following pyrophosphate catalysts ($Mn_2P_2O_7$, $Ni_2P_2O_7$, CeP_2O_7, $Mg_2P_2O_7$, ZrP_2O_7, $Ba_2P_2O_7$, $V_4(P_2O_7)_3$ and $Cr_4(P_2O_7)_3$) were prepared from their respective precursors (either nitrate of chloride form). Pure anhydrous sodium pyrophosphate ($Na_4P_2O_7$ was obtained from BDH, Germany) was added to an aqueous solution of the metal nitrate or metal chloride precursors to prepare the above mentioned metal pyrophosphate catalysts. The obtained precipitates were washed and then dried in an oven at 110 °C for 72 h. The catalysts powders were calcined in air at 600 °C for 3 h. Each calcined sample was pressed into pellets, crushed, and sieved into 20–40 mesh granules. The infrared spectra of the prepared catalysts were collected using a portage-460 Nicolet FTIR instrument before and after the reaction. The pore volume, average pore diameter and catalyst surface area were determined using Micromeritics ASAP-2000. X-ray diffraction was performed on a Philips PW diffractometer with Cu Kα radiation. The diffractometer was operated in the scanning mode with the step size of 0.04° and accounting time of 1 s.

2.2. Catalysts testing

The pyrophosphate catalysts were tested in a fixed-bed, quartz laboratory reactor, operated at atmospheric pressure. The experimental reaction temperature range was 400–600 °C and the feed contained 26.5% isobutane, 6.2% oxygen and the balance was helium. The three gases were of high purity (about 99.99%) obtained from Linde Co. These gases, which were delivered from cylinders at laboratory temperature, passed through microfilters for additional purification and metered by Omega electronic mass flow controllers before entering the reactor preheat zone.

Figure 1 shows the experimental setup of the catalytic reaction system used in this study. The reactor was a 7 mm internal diameter (id) tapered to a 2 mm id to ensure very rapid removal of the gases from the reaction zone, thus, minimizing possible gas phase reactions. 1 g of the 20–40 mesh size catalyst (occupying around 2.1 cm^3 of reactor volume) was placed in the reaction zone of the reactor and supported on quartz wool directly above the junction of the reaction zone with the bottom of the reactor. The temperature of the catalyst bed was monitored by a thermocouple placed on the reactor wall from outside. Omega temperature controllers were used to monitor the temperature. The actual temperature of the catalyst bed was calibrated in a separate experiment using a second thermocouple positioned in the center of the catalyst bed. This represents the reaction temperature reported in this work. In each case, the catalyst was pretreated in a mixed stream of oxygen and helium for 1 h at 400 °C. After the pretreatment, a total flow of 75 cm^3/min of the reactant gases was passed through the reactor at each desired temperature.

A gas chromatograph (HP 6890) was used for on-line analysis of both the feed and the product streams. The products passed directly through a heat-traced line to the GC sampling valve. The hydrocarbons and oxygenates were separated by HP-plot capillary column connected to a FID detector. Whereby, the permanent gases were separated by MS and Hayesep-R packed columns connected to a TCD detector. Triplicate runs of each experiment were conducted. The values reported in the paper are average values which varied by ±5% between runs. Carbon balance was in the range of 98 ± 2%.

3. Results and discussion

Table 1 shows the BET surface area, the pore volume and the average pore diameter. The CeP_2O_7 and ZrP_2O_7 have higher surface area compared to other pyrophosphate catalysts. While $Mn_2P_2O_7$, $V_4(P_2O_7)_3$, $Ni_2P_2O_7$ and $Mg_2P_2O_7$ have small surface areas. Among the pyrophos-

Table 1
Some physio-chemical properties of the pyrophosphate catalysts.

Sample	Total (BET) surface area (m^2/g)	Pore volume (cm^3/g)	Average pore diameter (Å)
CeP_2O_7	49.0	55.5	358.57
$Mn_2P_2O_7$	5.6	0.035	264.74
$V_4(P_2O_7)_3$	0.4	0.0039	558.45
ZrP_2O_7	47.3	0.132	56.02
$Ni_2P_2O_7$	1.5	0.01	108.98
$Mg_2P_2O_7$	0.22	0.018	575.18

Table 2
Catalytic reaction of isobutane over CeP_2O_7 at reaction temperatures of 500 and 550 °C.

	500 °C	550 °C
Conversion (%)		
C_4H_{10}	20.5	39.8
O_2	89.7	99.5
Product selectivity (%)		
C_4H_8	70.8	51.2
C_3H_6	14.0	23.9
C_2H_6	0.0	0.5
C_2H_4	0.3	1.8
CH_4	3.5	10.1
CO_2	2.9	5.2
CO	8.5	7.2
Oxygenates	Traces	Traces
Carbon balance (%)	99.1	97.3

phate catalysts used in this work only CeP_2O_7 shows high pore volume.

A typical product distribution in oxidative dehydrogenation of isobutane over pyrophosphate catalysts is shown in table 2 for CeP_2O_7. It is clear from the table that as the reaction temperature is increased from 500 to 550 °C, the isobutane conversion nearly doubles (from 20.5 to 39.8%) while almost complete conversion of oxygen is achieved at 550 °C. The selectivity towards isobutene formation drops from 70.8 to 51.2% and so does the C_{3+} (i.e., isobutene + propene: two important raw materials in the petrochemical industry) selectivity (it decreases from 84.8 to 75.1%).

Figure 2 (a) and (b) shows the isobutane conversion and isobutene selectivity obtained with the tested catalysts at 500 and 550 °C, respectively. The highest isobutane conversion (33.5%) was obtained with the vanadium pyrophosphate catalyst (denoted V in the figures) at 500 °C, however, the isobutene selectivity is lowest (47.2%). At 500 °C, the cerium pyrophosphate (CeP_2O_7) catalyst gave the highest yield and isobutene selectivity (70.8%) at an isobutane conversion of 20.5%. The same catalyst showed third highest conversion after V and Mn. Takiat et al. [7] recently reported a 78.7% isobutene selectivity at isobutane conversion of 4.1% for $CePO_4$ at 500 °C. It is worthy to mention here that in addition to the use of cerium phosphate instead of pyrophosphate, the isobutane to oxygen ratio in the feed for the Takita et al. [7] study was 15 : 1 whereas in this study 4 : 1. From table 2 and figure 2 it can be noticed that increasing the reaction temperature from 500 to 550 °C re-

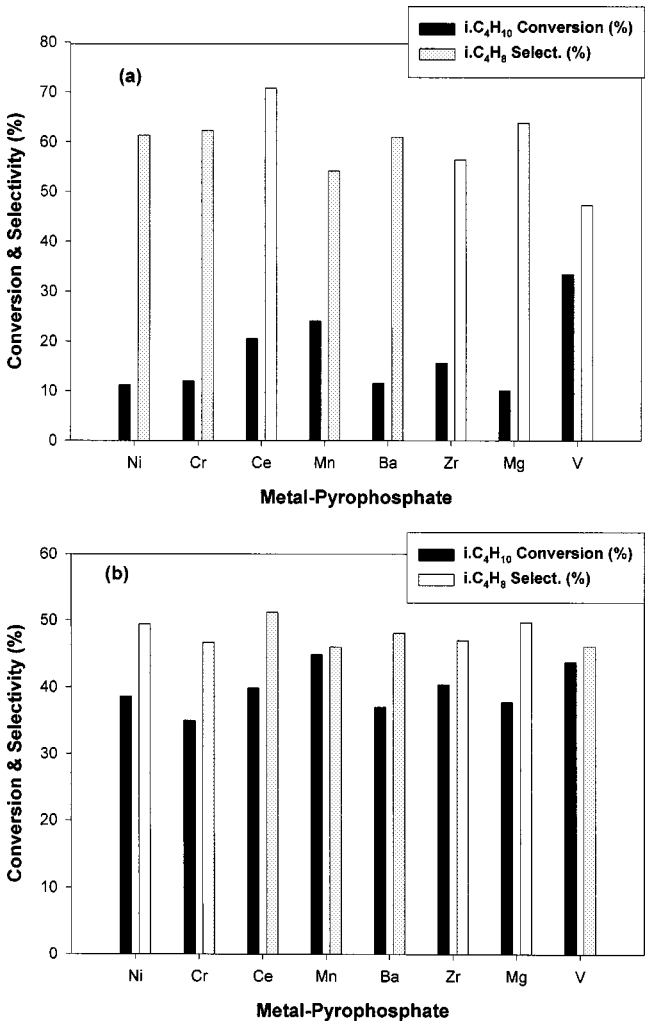

Figure 2. Isobutane conversion (%) and isobutene selectivity (%) for different metal pyrophosphates at (a) 500 and (b) 550 °C.

sults in higher isobutane conversions and lower isobutene selectivity to the benefit of cracking products and CO_x formation. At 500 °C, the vanadium pyrophosphate (V) catalyst gave the highest isobutane conversion (33%) followed by the manganese pyrophosphate (Mn) with 24% conversion. However, the same tendency was not observed at 550 °C due to the influence of the homogeneous gas phase reaction. Selectivity differences between these catalysts become also narrower. This indicates significant participation of homogeneous gas phase reactions. Previous studies [5] on the pyrophosphate system rank the nickel pyrophosphate to be the best amongst the Ni, Ag, Zn, Mg, Cr, Co, Mn and Sn catalysts. This is not confirmed under the conditions applied in our study. $Ni_2P_2O_7$ catalyst gave a 49.4% selectivity at a 38.6% conversion at 550 °C. This value is very close to Cr, Mn or Mg selectivities.

Figure 3 (a) and (b) compares the sum of the selectivities of isobutene and propene to that of carbon monoxide and carbon dioxide at 500 and 550 °C, respectively. From figure 3(a), it can be noticed that all tested pyrophosphate catalysts at 500 °C show high selectivities (78–90%) towards

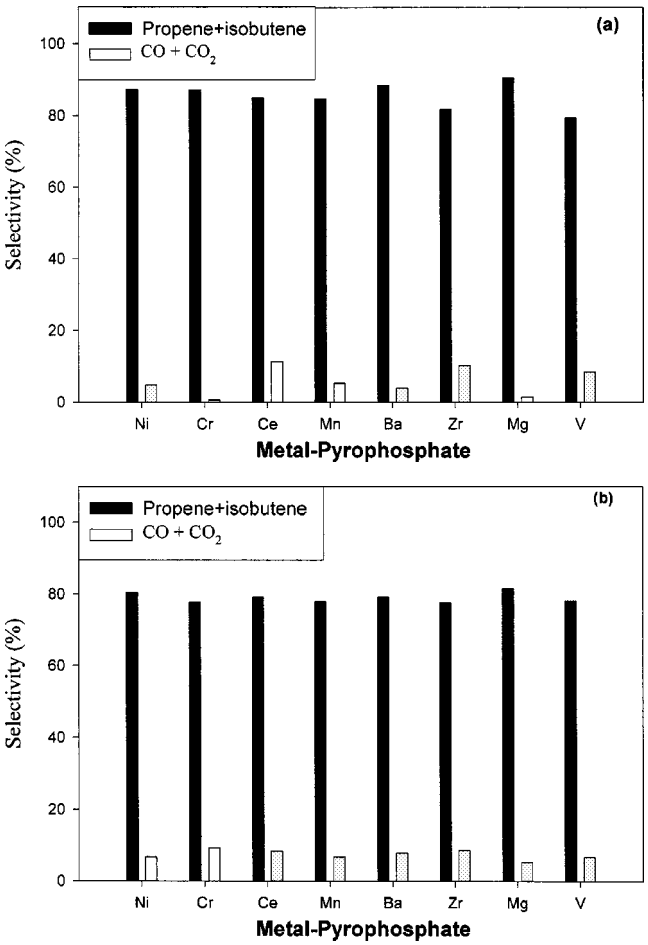

Figure 3. Comparison of ($C_4H_8 + C_3H_6$) selectivity to ($CO + CO_2$) selectivity at (a) 500 and (b) 550 °C.

C_{3+} products. The lowest propylene selectivity is obtained with the CeP_2O_7 catalyst with 14 and 23.9% at 500 and 550 °C, respectively. For all other catalysts, propylene selectivity was in the range of 25–33%. $V_4(P_2O_7)_3$ showed the highest propylene selectivity (33%) at 500 °C. Propylene selectivity can be correlated with the crack property of the catalyst which is attributed usually to the function of acidic sites. Takita et al. [6,7] studied the acidic properties of pyrophosphate and phosphate catalysts using the temperature-programmed desorption of NH_3. All of these catalysts showed acidic properties. Propylene was also observed with these catalysts. The isobutene formation showed relatively good correlation with the acidic properties of the catalysts. It is interesting to notice that the propylene selectivity at 550 °C is almost equal for all tested catalysts. In addition, oxygen was completely consumed by these catalysts. This reveals that at 550 °C the results are partly influenced by pure dehydrogenation reactions. Therefore, meaningful conclusions about actual catalytic properties cannot be drawn from the results at this temperature.

Insignificant amounts of oxygenates were detected. In a previous study, drastic drops in oxygenates formation from 77.2 to 2.9% with increase of reaction temperature from

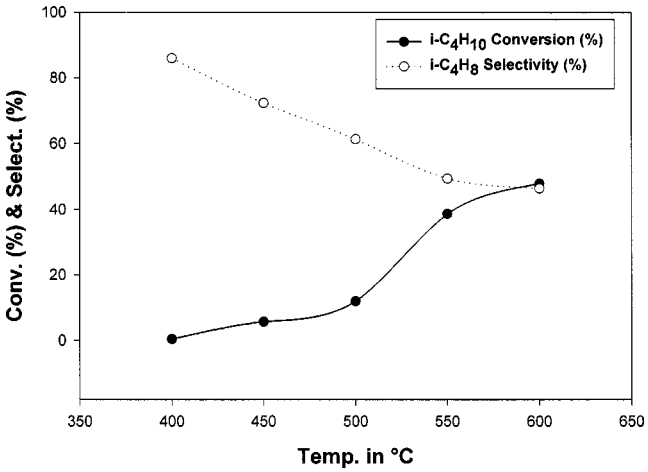

Figure 4. Effect of reaction temperature on conversion and selectivity for $Ni_2P_2O_7$ catalyst.

450 to 550 °C were observed [5,6]. In figure 3(a), compared to other catalysts, V, Zr and Ce pyrophosphate catalysts showed higher tendency towards the formation of total oxidation products. However, cerium-containing catalysts are more selective towards isobutene compared to Zr and V. It is interesting to note also that the sum of selectivities of CO, CO_2 and CH_4 is approximately equal to that of propene. This indicates that total oxidation products CO and CO_2 are formed from an active C_1 species, resulting from isobutane-crack reaction to produce propylene, and not as a result of further oxidation of C_4 oxygenates. This confirms the proposition that the following two reactions may proceed during selective ODH of isobutane:

$$i\text{-}C_4H_{10} + \tfrac{1}{2}O_2 \rightarrow i\text{-}C_4H_8 + \tfrac{1}{2}H_2O$$

$$i\text{-}C_4H_{10} \xrightarrow{O_2} C_3H_6 + CO, CO_2 \text{ or } CH_4$$

The effect of reaction temperature on isobutane conversion and isobutene selectivity is shown in figure 4 for the $Ni_2P_2O_7$ catalyst. It can be noticed from the figure that as the reaction temperature increases from 400 to 500 °C, the isobutane conversion slowly increases but the isobutene selectivity rapidly decreases. Further increase of temperature up to 600 °C results in a sharp increase of conversion up to about 48% and in a slower decrease of isobutylene selectivity to a final value of 50%. It is worthy to mention here again that at 550 °C, the oxygen conversion is very close to 100% which raises the possibility of homogeneous gas phase reactions. It is clear from the figure that as the reaction temperature is increased, the conversion increases but the selectivity decreases. The decrease of isobutene selectivity with reaction temperature contradicts the findings of Takita et al. [5–7] which indicates an increase of both selectivity and conversion with reaction temperature. We attribute this behaviour to the differences in feed composition (15 : 1 for Takita et al., and 4 : 1 in this study, as mentioned previously). The contradictory effect of reaction time seems to be less important, especially when

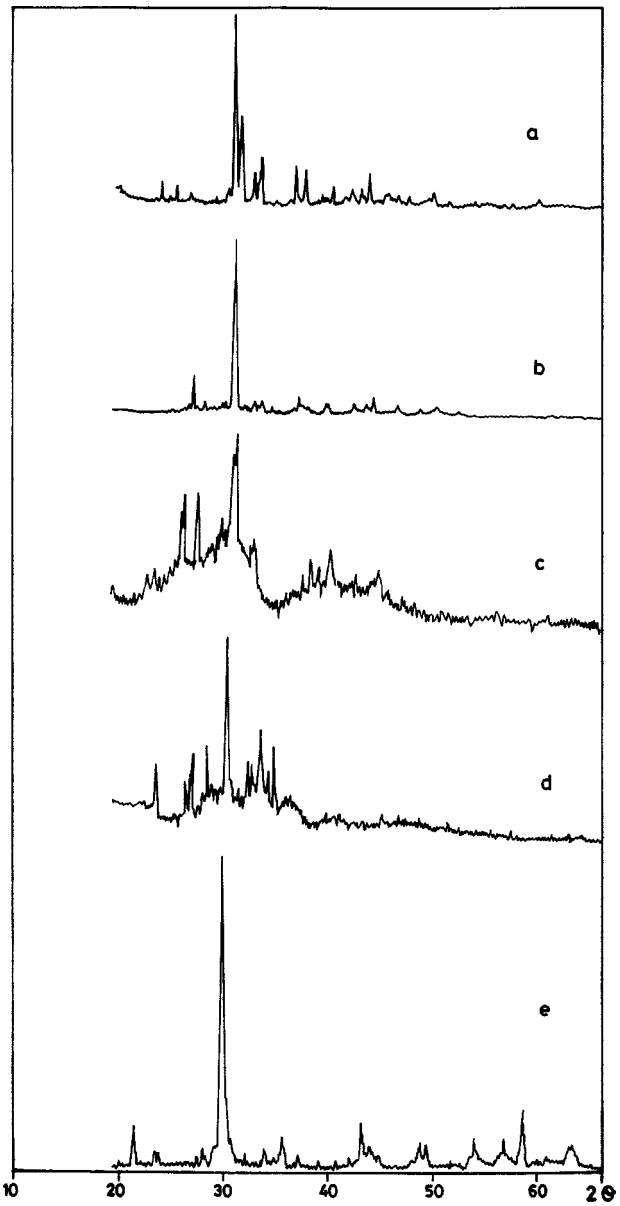

Figure 5. X-ray diffraction patterns for pyrophosphate catalysts: (a) $Mn_2P_2O_7$, (b) $Mg_2P_2O_7$, (c) ZrP_2O_7, (d) $V_4(P_2O_7)_3$ and (e) $Ni_2P_2O_7$.

taking into account the isobutane conversion was limited to 11% at 550 °C in both cases.

Typical X-ray diffraction patterns of pyrophosphate catalysts are displayed in figure 5. These diffractograms confirmed the formation of a pyrophosphate phase on the catalysts. Figure 6 shows the X-ray diffraction patterns of some representative pyrophosphate catalysts before and after the reaction. This figure indicates that the pyrophosphate catalysts did not suffer any structural modifications after the reaction.

$Ni_2P_2O_7$, $Mn_2P_2O_7$ and CeP_2O_7 catalysts have been analyzed using FT-IR before and after the reaction. These catalysts were selected for FTIR analysis due to their better performance compared to other pyrophosphate catalytic systems used in this work. In figure 7 two spectra are illustrated for each catalyst. For each set, the spectrum on the

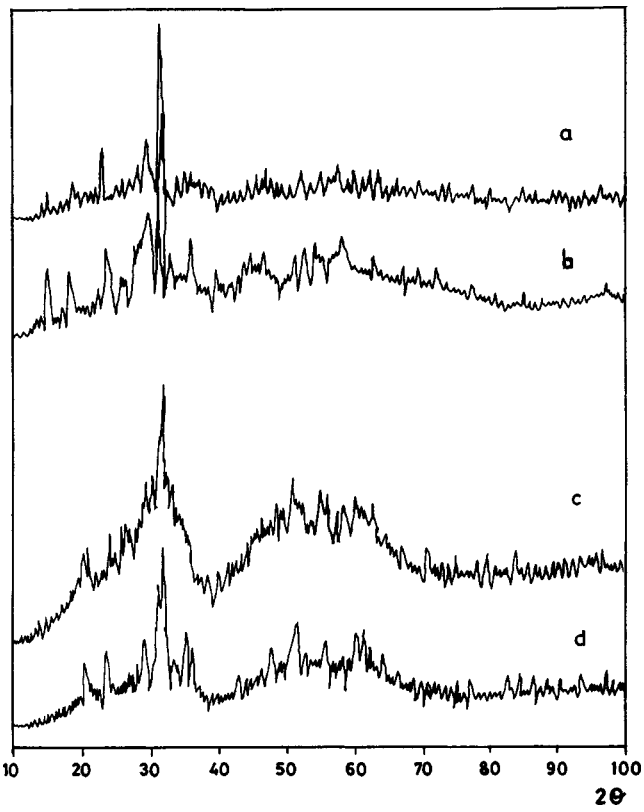

Figure 6. X-ray diffraction patterns for $V_4(P_2O_7)_3$: (a) calcined and (b) spent; and ZrP_2O_7: (c) calcined and (d) spent.

top belongs to a calcined catalyst sample (before the reaction) while the spectrum underneath it belongs to the same catalyst after the reaction. As a common observation, for all used catalysts the peaks detected in the range of 2500–3500 cm^{-1} are OH peaks. Most likely these peaks are adsorbed O–H in the stretch vibrational mode. The P_2O_7 group pattern appeared in the range of 900–1200 cm^{-1}, as shown in all the spectra. In the FTIR spectra (figure 7 (A) and (B)) for CeP_2O_7, a new peak was detected at a wave number of 1280 cm^{-1} after the reaction. This peak could be attributed to a single bond stretching –C–. The P_2O_7 group pattern becomes more intensive after the reaction. In the FTIR spectra (figure 7 (C) and (D)) for $Mn_2P_2O_7$, another new peak was detected at a wave number of 1380 cm^{-1}. This peak was correlated to a deformation H–C–H group. In contrast to CeP_2O_7, P_2O_7 in spectrum (D) is less separated. The FTIR spectra (figure 7 (E) and (F)) for $Ni_2P_2O_7$ show practically the same pattern before and after the reaction. These spectra indicate that the involvement of P_2O_7 group and adsorption of hydrocarbon species in the same oxidative dehydrogenation reaction is different on the tested catalysts. In this case metal property seems to be critical.

4. Conclusions

The following pyrophosphate catalysts ($Mn_2P_2O_7$, $Ni_2P_2O_7$, CeP_2O_7, $Mg_2P_2O_7$, ZrP_2O_7, $Ba_2P_2O_7$, $V_4(P_2O_7)_3$ and $Cr_4(P_2O_7)_3$) were used for oxidative dehydrogenation

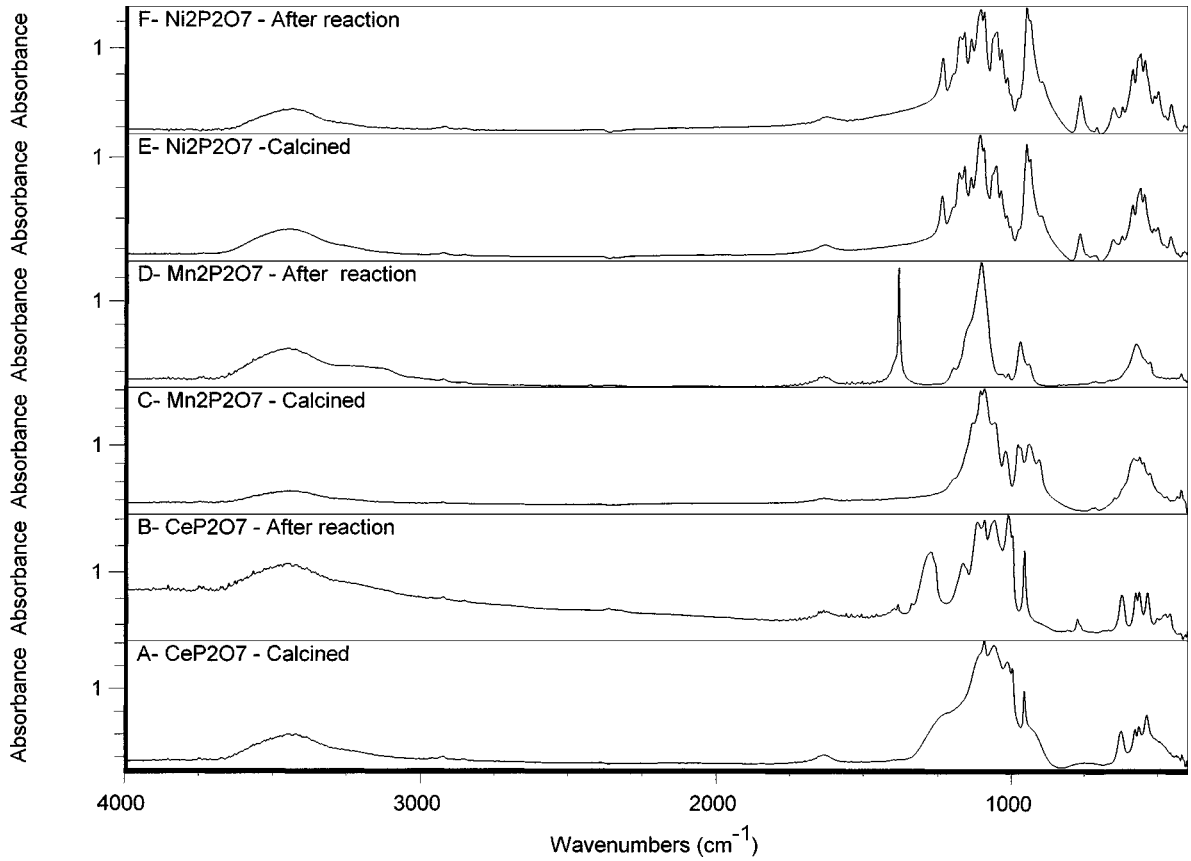

Figure 7. FT-IR spectra of CeP_2O_7 (A, B), $Mn_2P_2O_7$ (C, D) and $Ni_2P_2O_7$ (E, F) catalysts calcined and after the reaction.

of isobutane to isobutene. At 500 °C, CeP_2O_7 is the catalyst that gives the highest isobutene yield and selectivity while $V_4(P_2O_7)_3$ is the most active. Increasing the reaction temperature results in higher isobutane conversion but lower isobutene selectivity and it also raises the possibility of homogeneous gas phase reactions. These catalysts exhibit cracking properties attributed to the acidity function of the pyrophosphate group mainly to produce propylene and methane or oxidation products CO and CO_2. No clear correlation was observed between isobutene formation and catalyst acidity. XRD diffractograms confirmed the initial formation of a pyrophosphate phase. The FTIR spectra revealed that the involvement of the pyrophosphate group and adsorption of hydrocarbon species is different for the tested catalysts.

Acknowledgement

The authors are very grateful to Saudi Basic Industries Corporation – Research and Technology Department (SABIC - R&T) for funding this project.

References

[1] P.N. Degannes and D.M. Ruthven, Canad. J. Chem. Eng. 57 (1979) 627.
[2] T. Tagawa, T. Hattori and Y. Murakami, J. Catal. 75 (1982) 66.
[3] K. Fujimoto and T. Kunugi, Ind. Eng. Chem. Prod. Res. Dev. 20 (1981) 319.
[4] G. Emig and H.H. Hofmann, J. Catal. 84 (1983) 15.
[5] Y. Takita, K. Kurosaki, Y. Mizuhara and T. Ishihara, Chem. Lett. (1993) 335.
[6] Y. Takita, K. Sano, K. Kurosaki, N. Kawata, H. Nishiguchi, M. Ito and T. Ishihara, Appl. Catal. A 167 (1998) 49.
[7] Y. Takita, K. Sano, K.T. Muraya, N.H. Nishiguchi, N. Kawata, M. Ito, T. Akbay and T. Ishihara, Appl. Catal. A 170 (1998) 23.
[8] S.R. Mirzabekova and A.Kh. Mamedov, Kinet. Katal. 35 (1994) 903.
[9] A.T. Bell, M. Boudart and B.D. Ensley, *Catalysis Looks to the Future* (National Academy Press, Washington, DC, 1992).
[10] M. Hoang, J.F. Mathews and K.C. Pratt, J. Catal. 171 (1997) 320.
[11] B. Grzybowska, J. Sloczynski, R. Grabowski, K. Weislo, A. Kozlowska, J. Stoch and J. Zielinski, J. Catal. 178 (1998) 687.
[12] P. Moriceau, B. Grzybowska, Y. Barbaux, G. Wrobrl and G. Hecquet, Appl. Catal. A 168 (1998) 269.
[13] W.D. Zhang, D.L. Tang, X.P. Zhou, H.L. Wan and K.R. Tsai, J. Chem. Soc. Chem. Commun. (1994) 771.
[14] R. Grabowski, B. Grzybowska, J. Sloczynski and K. Weislo, Appl. Catal. A 144 (1996) 335.
[15] P.M. Michalakos, M.C. Kung, I. Jahan and H.H. Kung, J. Catal. 140 (1993) 226.
[16] F. Cavani, C. Comuzzi, G. Dolcetti, E. Etienne, R.G. Finke, G. Selleri, F. Trifirò and A. Trovarelli, J. Catal. 160 (1996) 317.
[17] C. Comuzzi, G. Dolcetti, A. Trovarelli, F. Cavani, F. Trifirò, J. Llorca and R.G. Finke, J. Catal. 36 (1996) 75.
[18] S. Albonetti, F. Cavani, F. Trifirò, M. Gazzano, M. Koutyrev, F.C. Aissi, A. Aboukais and M. Guelton, J. Catal. 146 (1994) 491.
[19] M. Fournier, A. Aouissi and C.R. Deltcheff, J. Chem. Soc. Chem. Commun. (1994) 307.